Bioconjugate Chemistry

Article

pubs.acs.org/bc

# Improved Metabolic Stability for $^{18}$F PET Probes Rapidly Constructed via Tetrazine *trans*-Cyclooctene Ligation

Ramajeyam Selvaraj,[†] Benjamin Giglio,[‡] Shuanglong Liu,[§] Hui Wang,[‡] Mengzhe Wang,[‡] Hong Yuan,[‡] Srinivasa R. Chintala,[†] Li-Peng Yap,[§] Peter S. Conti,[§] Joseph M. Fox,*[,†] and Zibo Li*[,‡]

[†]Brown Laboratories, Department of Chemistry and Biochemistry, University of Delaware, Newark, Delaware 19803, United States

[‡]Department of Radiology and Biomedical Research Imaging Center, University of North Carolina at Chapel Hill, Chapel Hill, North Carolina 27599, United States

[§]Molecular Imaging Center, Department of Radiology, University of Southern California, Los Angeles, California 90033, United States

Supporting Information

**ABSTRACT:** The fast kinetics and bioorthogonal nature of the tetrazine *trans*-cyclooctene (TCO) ligation makes it a unique tool for PET probe construction. In this study, we report the development of an $^{18}$F-labeling system based on a $CF_3$-substituted diphenyl-*s*-tetrazine derivative with the aim of maintaining high reactivity while increasing in vivo stability. c(RGDyK) was tagged by a $CF_3$-substituted diphenyl-*s*-tetrazine derivative via EDC-mediated coupling. The resulting tetrazine-RGD conjugate was combined with a $^{19}$F-labeled TCO derivative to give HPLC standards. The analogous $^{18}$F-labeled TCO derivative was combined with the diphenyl-*s*-tetrazine-RGD at $\mu$M concentration. The resulting tracer was subjected to in vivo metabolic stability assessment, and microPET studies in murine U87MG xenograft models. The diphenyl-*s*-tetrazine-RGD combines with an $^{18}$F-labeled TCO in high yields (>97% decay-corrected on the basis of TCO) using only 4 equiv of tetrazine-RGD relative to the $^{18}$F-labeled TCO (concentration calculated based on product's specific activity). The radiochemical purity of the $^{18}$F-RGD peptides was >95% and the specific activity was 111 GBq/$\mu$mol. Noninvasive microPET experiments demonstrated that $^{18}$F-RGD had integrin-specific tumor uptake in subcutaneous U87MG glioma. In vivo metabolic stability of $^{18}$F-RGD in blood, urine, and major organs showed two major peaks: one corresponded to the Diels–Alder conjugate and the other was identified as the aromatized analog. A $CF_3$-substituted diphenyl-*s*-tetrazine displays excellent speed and efficiency in $^{18}$F-PET probe construction, providing nearly quantitative $^{18}$F labeling within minutes at low micromolar concentrations. The resulting conjugates display improved in vivo metabolic stability relative to our previously described system.

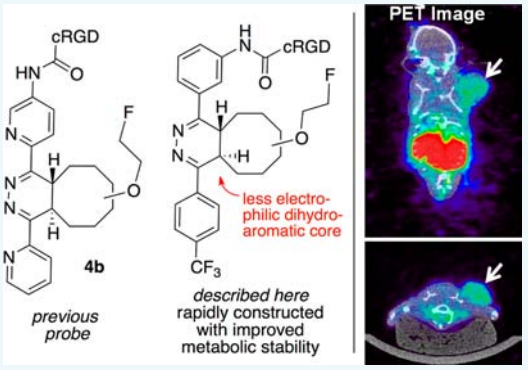


## INTRODUCTION

Positron emission tomography (PET) is a powerful and highly sensitive imaging technology with the capacity to observe metabolic processes and track radiolabeled biomolecules in vivo.[1] Of the various positron emitting radionuclides, $^{18}$F finds most the extensive use due to its clinically attractive half-life ($t_{1/2}$ = 110 min) and high positron efficiency ($\beta^+$ = 99%). To date, clinical applications of PET have largely involved small molecule probes such as $^{18}$F-2-deoxy-2-fluoroglucose.[2,3] Currently, there is great interest in the development of peptidic and protein-based probes for $^{18}$F PET imaging, with a correlated need to develop methods for bioligand probe construction. New methods for probe construction must operate efficiently within the constraints of $^{18}$F-labeling chemistry, which include the limited nucleophilicity and short half-life of fluoride and the need to efficiently conjugate molecules at low concentrations relevant to radiochemical experimentation.

A variety of $^{18}$F-labeled synthons have been developed and successfully applied to a host of peptides and proteins for $^{18}$F-PET probe construction. The utility of many $^{18}$F PET probes is hindered by multistep probe syntheses where $^{18}$F is carried through multiple chemical intermediates—a major limitation given the technically demanding nature of $^{18}$F radiochemistry. For the conjugation of $^{18}$F to the biological ligand, peptides or proteins are often used in large excess in order to obtain reasonable yields for $^{18}$F attachment. Additionally, $^{18}$F-tagged proteins or large peptides are often inseparable from their unlabeled precursors which can compromise the signal through competitive inhibition and result in low specific activity. Furthermore, sacrificing milligram quantities for labeling reactions is impractical for peptides or proteins that are not available in large quantity. Greatly needed are efficient and

**Received:** October 26, 2014
**Published:** February 13, 2015





DOI: 10.1021/acs.bioconjchem.5b00089
*Bioconjugate Chem.* 2015, 26, 435–442

robust methods for labeling proteins and peptides by $^{18}$F at low concentrations.

In 2008, we described methods for synthesizing *trans*-cyclooctene derivatives[4] and applying them in fast bioorthogonal reactions with tetrazines.[5] With strained TCO derivatives, rate constants of $k_2 > 10^6$ M$^{-1}$ s$^{-1}$ have been measured.[6−9] Concurrent with the initial study of TCO, several groups described reactions of tetrazines with derivatives of norbornene[10] or the Reppe anhydride,[11] with a measured rate constant of $k_2 = 1.9$ M$^{-1}$ s$^{-1}$ at 20 °C in PBS for norbornene conjugation. Recently, cyclopropenes,[12,13] cyclooctynes,[6,14,15] and terminal alkenes[16] have also been used as dienophiles for tetrazine ligation. While each of these dienophiles offers complementary advantages, TCO derivatives display the fastest rate constants.

The tetrazine-TCO ligation has become broadly used for research in nuclear medicine including applications in pretargeted imaging,[17−19] and studies have been directed toward optimizing and improving the pharmacokinetics and pharmacodynamics for systems based on dipyridyl-*s*-tetrazine and monoaryltetrazines.[7,17−25] In 2010, Robillard first showed that the tetrazine ligation method could be applied in a pretargeted antibody using single photon emission computed tomography (SPECT).[23] More recently, Robillard has described factors that contribute to the in vivo stability of TCOs toward isomerization,[7] and clearing agents have been developed that improve tumor-to-blood (125-fold) ratios.[22] Weissleder has shown that polymer modified tetrazines can be used for in vivo bioorthogonal labeling and PET imaging using an $^{18}$F-labeled TCO derivative.[20] More recently, Weissleder and Lewis reported a pretargeting approach for PET imaging based on this method and demonstrated dramatically reduced nontargeted organ uptake.[24] Recently, the reaction of a $^{11}$C-labeled tetrazine with a TCO derivative was described,[26] and Kuntner and Mikula described the development of an $^{18}$F-labeled tetrazine with favorable pharmacokinetic properties.[25]

In 2010, we developed a radiolabeling method for bioconjugation based on the Diels−Alder reaction between dipyridyl-*s*-tetrazines and an $^{18}$F-labeled *trans*-cyclooctene.[27] As shown in Figure 1, $^{18}$F-labeled TCO **2** could be obtained in high radiochemical yield (71%) by combining nosylate **1** with $^{18}$F-fluoride (100 mCi). $^{18}$F-**2** is an effective reagent for creating $^{18}$F-labeled probes within seconds at low micromolar concentrations, and we have used this reagent to make cyclic RGD (cRGD) and VEGF protein conjugates for cancer imaging[28,29] and exendin-4 conjugates for applications in insulinoma imaging and diabetes monitoring.[30] Notably, these conjugates were synthesized without using a large excess of the peptidic labeling precursor (Figure 1b). Avoiding excess labeling precursor is critically important for proteins and large polypeptides such as exendin-4 (MW 4775), where the labeled and unlabeled peptide are not readily separable, and unlabeled peptide can significantly decrease signal due to competitive inhibition.[30] Weissleder and Lewis have also used $^{18}$F-**2** in a number of applications including a recent demonstration of pretargeted imaging.[24]

An important factor that has not received significant attention is the metabolic stability of tetrazine−TCO conjugates. Dipyridyl-*s*-tetrazine-based probes with good pharmacokinetic properties have been constructed through conjugation to large peptides (exendin-4)[30] or by including PEG-spacers in antibody-pretargeting studies.[7,22,23] We also described that $^{18}$F-*trans*-cyclooctene **2** undergoes very rapid

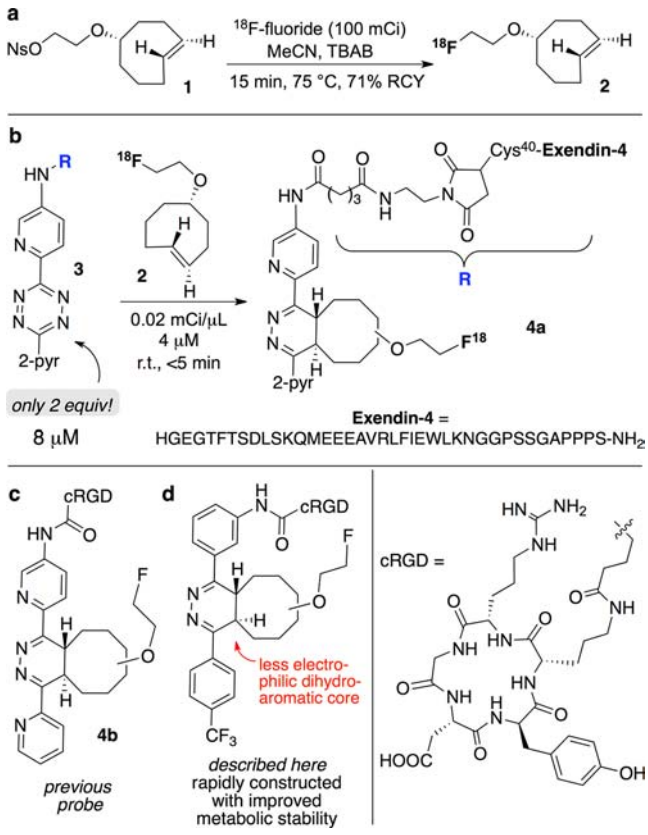


**Figure 1.** (a) Synthesis of $^{18}$F-TCO **2**. (b) Rapid $^{18}$F-labeling of a 4.8 kDa peptide takes place rapidly at low concentration using only a 2-fold excess of the peptide precursor. (c) Probe **4b** has been used to image U87MG tumors in mice. (d) A new probe that can also be constructed rapidly and used for U87MG tumor imaging in mice with the added benefit of improved metabolic stability.

conjugation with a dipyridyl-*s*-tetrazine-cRGD construct, and the resulting isomeric conjugates **4b** can be used to image tumors in mice (Figure 1c). Here, a relatively high level of organ uptake in the liver and kidneys was observed, presumably due to the hydrophobic nature of the probe. Because of the high residence time in the liver, we expected that this system would provide a good platform to test and improve the metabolic stability of tetrazine-based probes. In our study on **4b**, an attempt to reisolate radioactive **4b** from the major organs, urine, and blood of a mouse was not unsuccessful, and only hydrophilic degradation products were observed by radio-HPLC analysis. We hypothesized that the imines of **4b**, flanked with electron withdrawing pyridines, may be susceptible to nucleophilic attack and thereby provide a possible handle for degradation. We also hypothesized that a conjugate (Figure 1d) with fewer electron withdrawing aromatic groups would be more stable. Here, we describe a 3,6-diphenyl-*s*-tetrazine derivative that displays fast conjugation rates toward $^{18}$F-**2** and gives conjugates with improved metabolic stability in an in vivo mouse study. $^{18}$F-labeling yields are discussed and the metabolic stability of the $^{18}$F-**2** tagged cRGD conjugate is described. The PET probe was evaluated for integrin $\alpha_v\beta_3$ imaging in U87MG tumor-bearing mice by microPET.

## RESULTS

**Chemistry.** The $CF_3$-substituted diphenyl-*s*-tetrazine **6**[35] was prepared by an improved two-step procedure and


DOI: 10.1021/acs.bioconjchem.5b00089
*Bioconjugate Chem.* 2015, 26, 435−442

elaborated by EDC coupling to cRGD derivative **7** (Figure 2a). To gauge the reactivity of derivatives of diaryltetrazine **6**, stopped flow kinetic analysis was used to measure the rate of the Diels–Alder reaction between tetrazine derivative **8** and equatorially substituted *trans*-cyclooctene derivative **9**, the precursor to $^{18}$F-**2** (Figure 2). The undecaethylene glycol side chain of **8** was added to enhance water solubility. In water/MeOH (6:4, v/v) at 25 °C, a second order rate constant $k_2$ = 1000 ± 100 $M^{-1}$ $s^{-1}$ was measured.

The cycloaddition reaction of tetrazine-cRGD **7** and $^{19}$F-**2** provided $^{18}$F-cRGD conjugates **10**, which were used as radiolabeling standards and for the integrin receptor binding assay. Consistent with the high reactivity of **8**, the pink color of tetrazine-cRGD **7** disappeared immediately upon mixing with $^{19}$F-**2**. The identity of the $^{19}$F-cRGD conjugates **10** were confirmed by LC-MS. As expected based on prior observation and a model study,[5,9,36] both aromatized conjugates **10b** were formed in addition to dihydropyridazine conjugates **10a** (Figure 3a,b). Collectively, we refer to the mixture of aromatic and dihydropyridazine conjugates as **10**.

**Radiochemistry.** $^{18}$F-labeled *trans*-cyclooctene ($^{18}$F-**2**) was produced using the protocol developed in our laboratories[27] and utilized in radiolabeling experiments with tetrazine-cRGD

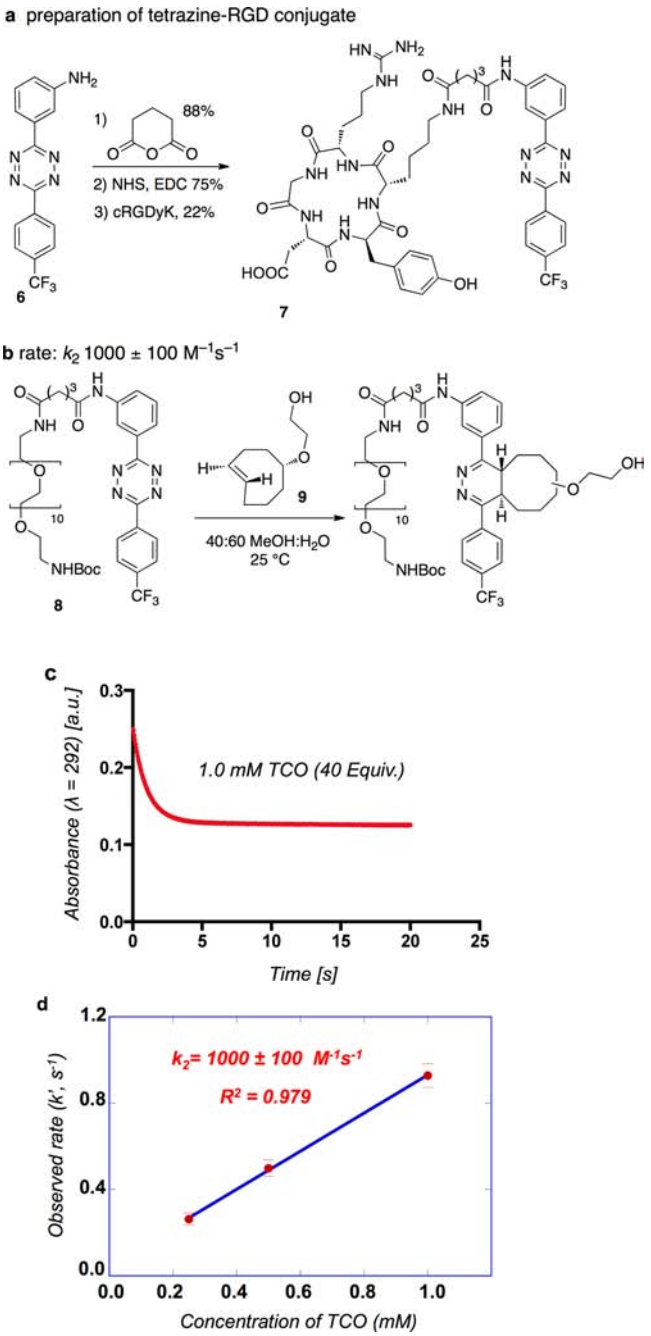


**Figure 2.** (a) Synthesis of a cRGD-diphenyl-*s*-tetrazine conjugate. (b) The rate of the conjugation of **8** with **9** was determined by stopped-flow kinetic analysis. (c) The exponential plot of the reaction of **8** (25 $\mu$M) and **9** (1.0 mM) in 40:60 MeOH:water was monitored at 292 nm. Data was recorded for 20 s at 298 K, with triplicate runs on three independent samples at three different concentrations (27 runs total). (d) The average of three observed rates $k'$ vs concentration of **9** for the reaction between **8** and **9**. Under these pseudo-first-order conditions the second-order rate constant ($k_2$) was determined by nonlinear regression to be 1000 ± 100 $M^{-1}$ $s^{-1}$.

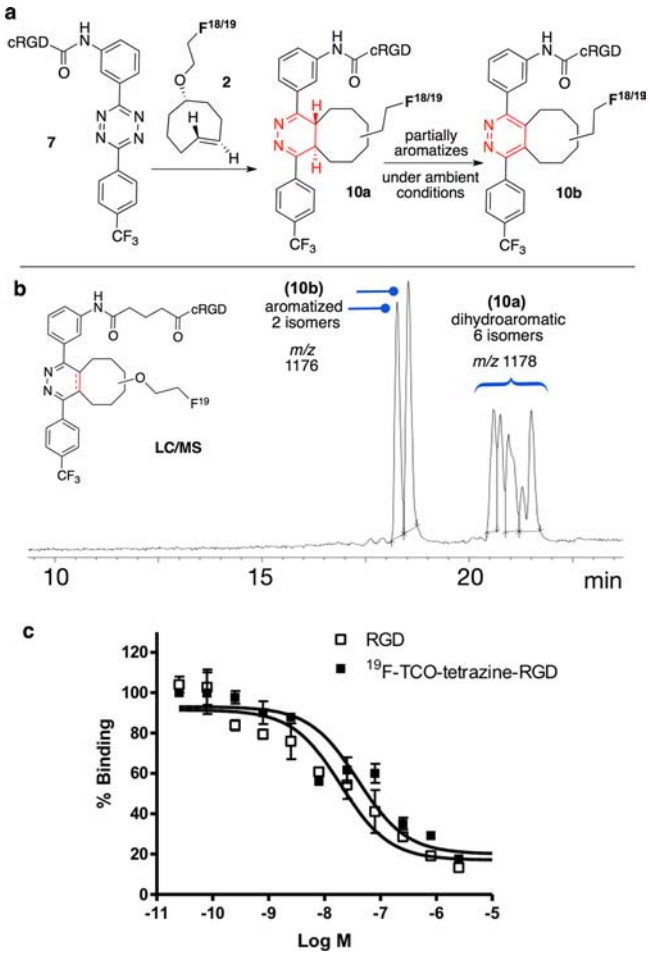


**Figure 3.** (a) Conjugation of a cyclic-RGD-tetrazine **7** with F-TCO **2** gives conjugates **10a**, which slowly oxidize to aromatic isomers **10b** under ambient conditions in aqueous solution. (b) LC/MS analysis of the Diels–Alder conjugate from $^{19}$F-**2** acquired after the sample had been allowed to stand overnight shows a mixture of aromatized and more slowly eluting dihydroaromatic products. Chromatographic resolution was higher and retention times longer in this LC/MS run than in radio-HPLC analyses (Figures 4, 5). (c) Cell-binding assay of c(RGDyK) and $^{19}$F-Diels–Alder conjugates **10** using U87MG cells (integrin $\alpha_v\beta_3$-positive human glioblastoma). The cell-binding affinity of the peptides was determined by performing competitive displacement studies with $^{125}$I-echistatin ($n$ = 3).



DOI: 10.1021/acs.bioconjchem.5b00089
*Bioconjugate Chem.* 2015, 26, 435–442

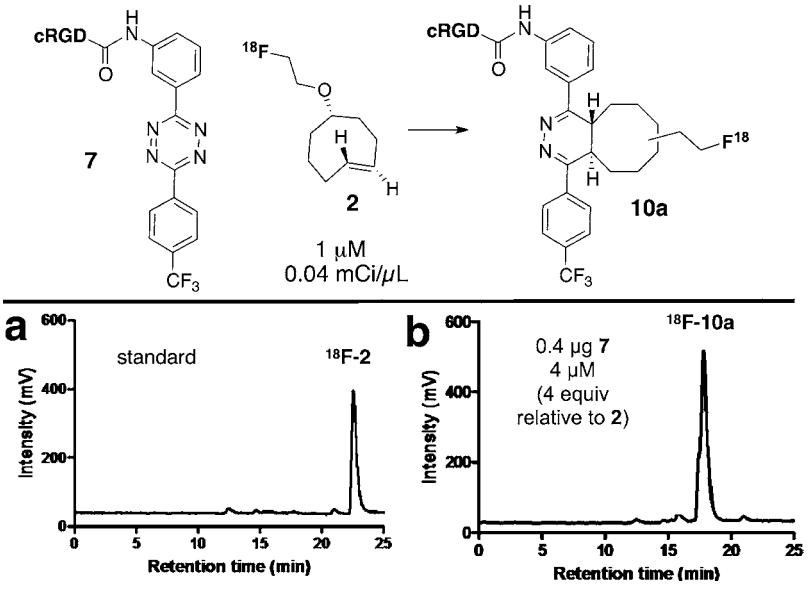


**Figure 4.** $^{18}$F labeling by $^{18}$F-**2** (1 $\mu$M) with differing concentrations of **7**. The product $^{18}$F-**10a** is a mixture of regioisomers. (a) HPLC standard of $^{18}$F-**2**. (b) 97% radiochemical yield with 4 equiv of **2**. The specific activity of $^{18}$F-**10** was determined to be 3.0 ± 1.0 Ci/$\mu$mol after purification by comparing the UV absorption with standard titration curve.

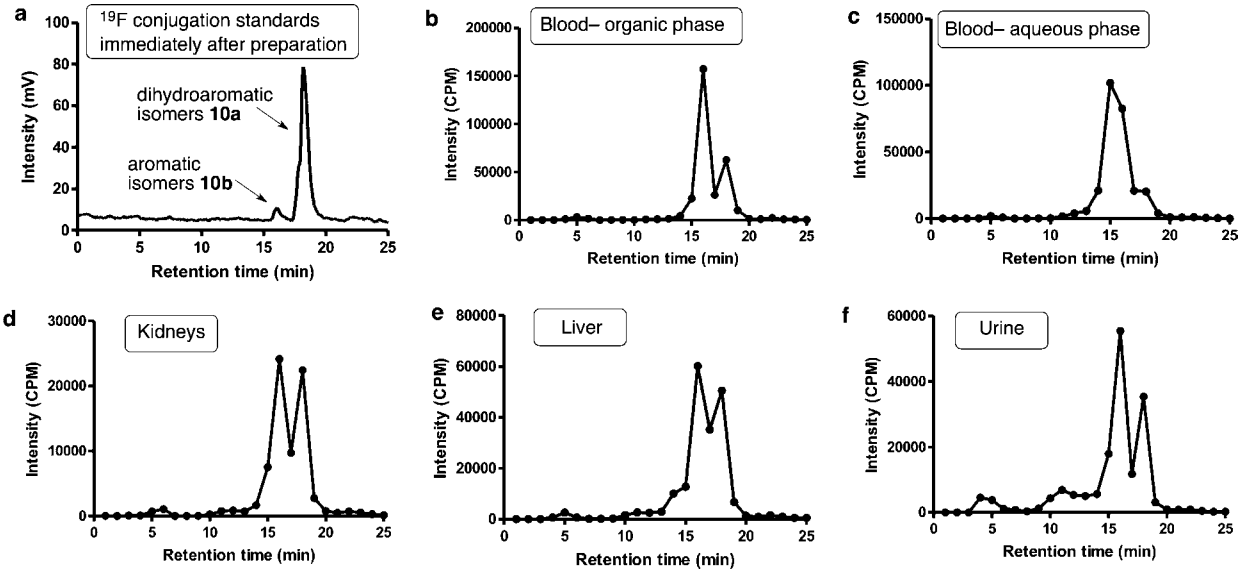


**Figure 5.** Metabolic stability of $^{18}$F-**10** in mouse blood and urine samples and in liver and kidney homogenates at 1 h after injection. Fractions were collected every minute and radioactivity measured by $\gamma$-counter. The radio-HPLC profile of $^{18}$F-**10** standard is also shown. In each of the metabolic extracts, two peaks were observed. One peak corresponded to dihydropyridizine isomers $^{18}$F-**10a**, and the other peak corresponded to isomers of pyridizine $^{18}$F-**10b**.

derivative **7** (Figure 4). With only a 4-fold excess of **7** (4 $\mu$M) relative to $^{18}$F-**2** (1 $\mu$M, calculated based on the specific activity of $^{18}$F-**10a**), a 97% radiochemical yield of $^{18}$F-**10a** was obtained (Figure 4b). The specific activity of $^{18}$F-**10** was determined to be 3.0 ± 1.0 Ci/$\mu$mol after purification by comparing the UV absorption with standard titration curve.

**Cell Integrin Receptor-Binding Assay.** Receptor-binding affinity studies of $^{19}$F-**10** and unmodified c(RGDyK) toward $\alpha_v\beta_3$ integrin were performed using $\alpha_v\beta_3$ integrin-positive U87MG cells. Binding on the cell membrane allows cross-linking and integrin receptor multimerization, through which multivalent binding and clustering of receptor is studied in the natural context of the integrin. We compared the receptor-binding affinity of $^{19}$F-**10** with that of unlabeled c(RGDyK) by performing competitive displacement studies with $^{125}$I-echistatin (Figure 3c). Both $^{19}$F-**10** and unmodified c(RGDyK) peptides inhibited the binding of $^{125}$I-echistatin to $\alpha_v\beta_3$ integrin−positive U87MG cells. The $IC_{50}$ values for $^{19}$F-**10** and c(RGDyK) were 39.8 ± 4.5 and 19.6 ± 3.2 nmol/L, respectively. Thus, the fluoride incorporation via tetrazine ligation into the cRGD peptide had minimal effect on binding affinity to the $\alpha_v\beta_3$ receptors.

**In Vivo Metabolism of $^{18}$F-10.** The metabolic stability of $^{18}$F-**10** was determined in mouse blood and urine and in liver and kidney homogenates at 2 h after tracer injection. The extraction efficiency of all organs was between 56% and 98%. The lowest extraction efficiency was found for the kidney homogenates and the highest extraction efficiency was from


DOI: 10.1021/acs.bioconjchem.5b00089
Bioconjugate Chem. 2015, 26, 435−442

blood sample. The intact probes were 75%, 51%, 57%, and 62% for blood, kidney, liver, and urine samples, respectively (Figure 5). The major metabolites correlate well with the aromatized product. These results showed that the new probe displayed significantly higher stability than previous dipyridyl analogues.[27,29]

**microPET Studies.** The localization of $^{18}$F-**10** in human U87MG tumor-bearing nude mice ($n$ = 5) was performed by multiple time-point static microPET scans. Figure 6a shows microPET images of a female mouse at different times after injection of 7.4 MBq (200 $\mu$Ci) of $^{18}$F-**10**. All microPET images were decay corrected. The tumor was clearly visualized with good contrast. Figure 6b shows the microPET images with a blocking dose of unlabeled c(RGDyK) peptide coinjection. The tumor uptake of the radio probe was clearly reduced. The microPET imaging study demonstrated high and specific binding of $^{18}$F-**10** to human U87MG tumors. Quantification of activity accumulation in the tumor and major organs (Figure 6c) was determined by biodistribution studies conducted 2 h post injection.

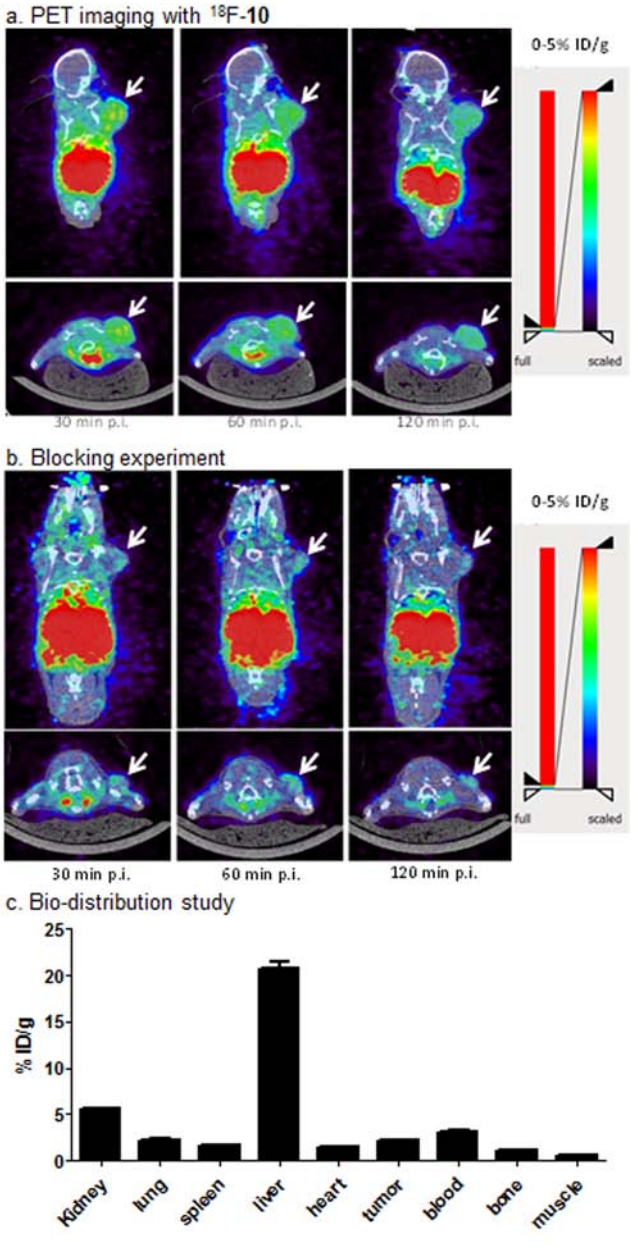


**Figure 6.** microPET images of athymic nude mice bearing U87MG tumor at 0.5, 1, and 2 h after injection of $^{18}$F-**10** (a) without or (b) with a blocking dose of $c$(RGDyK) peptide (10 mg/kg body weight) ($n$ = 5). Tumors are indicated by arrows. (c) Biodistribution study of $^{18}$F-**10** in nude mice bearing U87MG tumor at 2 h p.i..

## DISCUSSION

Although dipyridyl-$s$-tetrazine conjugates with $^{18}$F-**2** can be created rapidly and efficiently, in prior studies on RGD-based imaging[29] we observed that these conjugates have only moderate metabolic stability in vivo. We hypothesized that a conjugate with fewer electron withdrawing phenyl groups would be more stable, and in line with prior observations may spontaneously oxidize to give aromatic pyridazine products that are also highly stable.[5,9] To test this hypothesis, we prepared the diphenyl-$s$-tetrazine derivatives **7** and **8** from precursor **6**. Compound **8** reacts with *trans*-cyclooctene derivative **9** in water/MeOH (6:4, v/v) at 25 °C with $k_2$ = 1000 ± 100 $M^{-1}$ $s^{-1}$. When compared under similar conditions, the rate of reactivity for the $CF_3$-substitituted tetrazine **8** falls within an order of reactivity of the faster dipyridyl-$s$-tetrazine derivatives **3**.[6,37]

Encouraged by the efficient reactivity of **8** with **9**, we reacted the cRGD-diphenyl-$s$-tetrazine derivative **7** with $^{19}$F-**2** to provide conjugate **10a**, a mixture of isomers (Figure 3a). In line with observations from model compounds,[36] we found that **10a** partially oxidized spontaneously in solution to provide aromatic **10b**. Shown in Figure 3b is the HPLC−MS trace of the Diels−Alder conjugate from **7** (10 $\mu$M) and $^{19}$F-**2** (10 $\mu$M) analyzed after standing overnight in aqueous solution. As expected,[5,9] in addition to peaks from the dihydroaromatic Diels−Alder adducts **10a** ($m/z$ 1176), we also observed the aromatized pyridizine adducts **10b** ($m/z$ 1178). As shown in Figure 3c, the receptor-binding affinity of **10** was compared to that of unlabeled c(RGDyK) by performing competitive displacement studies with $^{125}$I-echistatin. The $^{19}$F-cRGD conjugate **10** was comparable to the unlabeled cyclic RGD peptide in its ability to inhibit the binding of $^{125}$I-echistatin to $\alpha_v\beta_3$ integrin-positive U87MG cells.

To study the stability of the $^{18}$F-labeled Diels−Alder conjugates, an in vivo metabolic study was carried out by injecting $^{18}$F-**10** into an athymic nude mouse that was sacrificed 2 h post injection. The organ uptake by the kidneys and liver for $^{18}$F-**10** (Figure 6) is similar to what was observed with dipyridyl-$s$-tetrazine-RGD construct **4b** (Figure 1c). As shown previously, the organ uptake was greatly reduced when the more hydrophilic probe **4a** based on the exendin-4 ligand (Figure 1b) was used to image a GLP-1R positive tumor in mice.[30] Similarly, we anticipate that the pharmacokinetic/pharmacodynamic properties of probes related to **4a** will readily be improved with protein-based probes, or with peptide-based probes where hydrophilic spacer molecules are employed. For the present study, to investigate the stability of the tetrazine-TCO conjugate in vivo, the organ uptake of $^{18}$F-**10** was considered advantageous as it allowed study of probe that had been retained in these organs. Thus, major tissues were collected and homogenized, and the activity was extracted and analyzed by HPLC (Figure 5). Fractions were collected each minute and radioactivity measured with the $\gamma$-counter. The average fraction of intact tracer was significantly improved relative to the first generation system **4b** (Figure 1c), where


DOI: 10.1021/acs.bioconjchem.5b00089
Bioconjugate Chem. 2015, 26, 435−442

only degradation products were observed by HPLC in similar attempts to recover radioactivity from blood, urine, and organs of the animal. For $^{18}$F-**10**, a hydrophilic byproduct was not observed by HPLC analysis, and the probe was detected with high fidelity in extracts from the kidneys, liver, blood, and urine. To ensure that there was not a hydrophilic byproduct in the homogenates, we also analyzed the aqueous phase from the blood sample. The HPLC profile was very similar to that from the organic phase. In each of the metabolic extracts, two peaks were observed. Upon comparison of the HPLC data (Figure 5) and LC/MS (Figure 3b) data with cold conjugates it was concluded that one peak corresponded to the dihydropyridizine isomers of $^{18}$F-**10a**, and the other peak to the aromatized isomers $^{18}$F-**10b**. One limitation of using $^{18}$F-**2** is the high number of isomeric conjugates that are formed upon conjugation with unsymmetrical tetrazines, which may present an issue for clinical translation. Efforts to ameliorate this issue by using higher symmetry cyclooctene derivatives are in progress.

$^{18}$F-**10** exhibited good metabolic stability in vivo, and injection of $^{18}$F-**10** into a U87MG mouse model resulted in an effective method for $\alpha_v\beta_3$ imaging. The integrin $\alpha_v\beta_3$ receptor specificity was confirmed by blocking experiments, in which unlabeled cRGD was administered prior to the injection of the $^{18}$F-**10** (Figure 6). Thus, this labeling system has improved product stability, and no defluorination of $^{18}$F-**10** was observed as no visible bone uptake was observed in any of the microPET scans. We also performed a PBS stability study on newly synthesized $^{18}$F-**10**. Around 28% of product got aromatized at 2 h post incubation (Figure S2).

A major advantage of the tetrazine ligation lies in the ability to enable fast reactivity at low micromolar concentrations within minutes and without an excess of either reactant. After demonstrating that the tetrazine **7** is robust and that conjugates with $^{18}$F-**2** have good stability in vivo, we explored the lower limit of concentration for the $^{18}$F labeling reaction. As benchmarks, the decay-corrected labeling yield was 35−45% when *N*-succinimidyl-4-$^{18}$F-fluorobenzoate was combined with an RGD derivative at 0.11 mM,[38] and 70% when an RGD derivative at 1.8 mM was labeled with $^{18}$F by Cu-catalyzed azide/alkyne cycloaddition.[39] By contrast, the tetrazine−TCO ligation reaction is nearly quantitative at a concentration that is more dilute by more than 3 orders of magnitude (Figure 4). Thus, a 97% radiochemical yield of $^{18}$F-**10** was obtained in 5 min when $^{18}$F-**2** (4 $\mu$Ci/$\mu$L, 1 $\mu$M) was combined with only 4 equiv of **7** (0.4 $\mu$g, 0.4 nmol, 4 $\mu$M). We believe that this combination of fast reactivity to yield metabolically stable conjugates should continue to enable applications in $^{18}$F-based labeling and imaging.

## CONCLUSION

A $CF_3$-substituted 3,6-diphenyl-*s*-tetrazine derivative displays fast conjugation rates toward $^{18}$F-2, providing that nearly quantitative $^{18}$F labeling was observed within minutes at low micromolar concentrations. This bioorthogonal ligation reaction was used to construct an $^{18}$F-cRGD conjugate, which was evaluated for integrin $\alpha_v\beta_3$ imaging in U87MG tumor-bearing mice by microPET. The conjugate was further shown to display improved metabolic stability in an in vivo mouse study.

## MATERIALS AND METHODS

All commercially available chemical reagents were used without further purification. The syringe filter and poly(ether sulfone) membranes (pore size, 0.22 $\mu$m; diameter, 13 mm) were obtained from Nalge Nunc International (Rochester, NY). $^{125}$I-Echistatin was purchased from PerkinElmer (Piscataway, NJ). c(RGDyK) was obtained from Peptides International (Louisville, KY). All HPLC conditions are gradient. HPLC methods, NMR spectra, and mass spectrometry details are listed in Supporting Information. MicroPET scans were performed on a microPET R4 rodent model scanner (Siemens Medical Solutions USA, Inc., Knoxville, TN), or a GE eXplore Vista.

**Chemistry.** Detailed synthetic procedures and characterization details are provided as Supporting Information.

**Stopped-Flow Kinetic Analysis.** The second-order rate constant was measured under pseudo-first-order conditions using an excess of TCO **9** by following the exponential decay of absorbance due to the tetrazine chromophore of **8** at 292 nm using an SX 18MV-R stopped-flow spectrophotometer (Applied Photophysics Ltd.). Thus, equal volumes of solutions of TCO **9** (0.50 mM, 1.0 mM, or 2.0 mM in 60:40 water:methanol) and tetrazine **8** (0.050 mM in 60:40 water:methanol) were mixed in the stopped flow device. The final concentration of **8** was 25 $\mu$M, and that of **9** was 0.25 mM, 0.50 mM, or 1.0 mM. At each concentration, kinetic data was repeated nine times (triplicate runs on three independent samples) at 298 K. Thus, 27 rate measurements were made. The rate constant was determined by nonlinear regression analysis using Prism (GraphPad Software, Inc.). The mean second-order rate constant under these conditions was measured to be 1000 ± 100 $M^{-1}$ $s^{-1}$.

**Radiochemistry.** The $^{18}$F-labeled TCO ($^{18}$F-**2**, Figure 1) was synthesized as reported.[27] A solution of 0.4 mCi (14.8 MBq) $^{18}$F-**2** in ethanol was added to different concentrations of tetrazine-cRGD **7** in DMSO (total volume 100 $\mu$L). After vigorous vortexing for 1 min at room temperature, the reaction was quenched with 1 mL 0.1% TFA in water and loaded onto a C-18 HPLC column to determine the labeling yield. With a loading of **7** at 4 $\mu$M, probe **10** was obtained with 97% labeling yield (Figure 4). For small animal study, the HPLC fraction containing$^{18}$F-**10** was collected and the HPLC eluent was removed using a rotary evaporator. $^{18}$F-**10** was reconstituted in 1 mL PBS and passed through a 0.22 $\mu$m syringe filter for animal injection.

**Cell Integrin Receptor-Binding Assay.** In vitro integrin-binding affinities and specificities of tetrazine-cRGD peptides were assessed via displacement cell binding assays using $^{125}$I-echistatin as the integrin-specific radioligand. Experiments were performed on the human glioblastoma U87MG cell line by modification of a method previously described.[31]

**Animal Models.** Animal procedures were performed according to a protocol approved by the UNC Institutional Animal Care and Use Committee. Human brain cancer carcinoma xenografts were induced by subcutaneous injection of $10^7$ U87MG cells into the right front leg of female athymic nude mice. Three weeks after inoculation of the tumor cells, when the tumor reached 0.4−0.6 cm in diameter, the mice were used for microPET experiments.

**Metabolic Stability.** The metabolic stability of $^{18}$F-**10** was evaluated in an athymic nude mouse bearing a U87MG tumor according a reported procedure.[32] Detailed procedures are included as Supporting Information.



DOI: 10.1021/acs.bioconjchem.5b00089
*Bioconjugate Chem.* 2015, 26, 435−442

**microPET Studies.** PET of tumor-bearing mice was performed on an eXplore Vista microPET/CT rodent model scanner using a reported method.[33,34] In brief, the mice were injected with 7.4 MBq of $^{18}$F-RGD conjugate **10** with or without a blocking dose of unlabeled RGD peptide via the tail vein and then anesthetized with 2% isoflurane and placed near the center of the FOV of the microPET where the highest image resolution and sensitivity are obtained.

## ■ ASSOCIATED CONTENT

### Supporting Information

Experimental procedures, spectral data for all new compounds, kinetic plots, and HPLC traces. This material is available free of charge via the Internet at http://pubs.acs.org.

## ■ AUTHOR INFORMATION


### Corresponding Authors

*E-mail: jmfox@udel.edu.

*E-mail: ziboli@med.unc.edu.

### Author Contributions

Ramajeyam Selvaraj, Benjamin Giglio, and Shuanglong Liu contributed equally to the research work.


### Notes

The authors declare no competing financial interest.

## ■ ACKNOWLEDGMENTS

This work was supported by NIH Grant Number P20 RR017716 from the COBRE Program of the NCRR, NIBIB (7R01EB014354-02), P30CA014089, P30-CA016086-35-37 from the National Cancer Institute, and UNC Radiology Department and BRIC. Spectra were obtained with instrumentation supported by NSF CRIF:MU grants: CHE 0840401 and CHE-0541775.

## ■ REFERENCES


(1) Czernin, J., and Phelps, M. E. (2002) Positron emission tomography scanning: current and future applications. *Annu. Rev. Med. 53*, 89−112.

(2) Gallagher, B. M., Fowler, J. S., Gutterson, N. I., MacGregor, R. R., Wan, C. N., and Wolf, A. P. (1978) Metabolic trapping as a principle of radiopharmaceutical design: some factors resposible for the biodistribution of [$^{18}$F] 2-deoxy-2-fluoro-D-glucose. *J. Nucl. Med. 19*, 1154−61.

(3) Reivich, M., Kuhl, D., Wolf, A., Greenberg, J., Phelps, M., Ido, T., Casella, V., Fowler, J., Hoffman, E., Alavi, A., et al. (1979) The [$^{18}$F]fluorodeoxyglucose method for the measurement of local cerebral glucose utilization in man. *Circ. Res. 44*, 127−37.

(4) Royzen, M., Yap, G. P., and Fox, J. M. (2008) A photochemical synthesis of functionalized *trans*-cyclooctenes driven by metal complexation. *J. Am. Chem. Soc. 130*, 3760−1.

(5) Blackman, M. L., Royzen, M., and Fox, J. M. (2008) Tetrazine ligation: fast bioconjugation based on inverse-electron-demand Diels-Alder reactivity. *J. Am. Chem. Soc. 130*, 13518−9.

(6) Lang, K., Davis, L., Wallace, S., Mahesh, M., Cox, D. J., Blackman, M. L., Fox, J. M., and Chin, J. W. (2012) Genetic Encoding of bicyclononynes and *trans*-cyclooctenes for site-specific protein labeling in vitro and in live mammalian cells via rapid fluorogenic Diels-Alder reactions. *J. Am. Chem. Soc. 134*, 10317−20.

(7) Rossin, R., van den Bosch, S. M., Ten Hoeve, W., Carvelli, M., Versteegen, R. M., Lub, J., and Robillard, M. S. (2013) Highly reactive *trans*-cyclooctene tags with improved stability for Diels-Alder chemistry in living systems. *Bioconjugate Chem. 24*, 1210−7.

(8) Selvaraj, R., and Fox, J. M. (2013) *trans*-Cyclooctene−a stable, voracious dienophile for bioorthogonal labeling. *Curr. Opin. Chem. Biol. 17*, 753−60.

(9) Taylor, M. T., Blackman, M. L., Dmitrenko, O., and Fox, J. M. (2011) Design and synthesis of highly reactive dienophiles for the tetrazine-*trans*-cyclooctene ligation. *J. Am. Chem. Soc. 133*, 9646−9.

(10) Devaraj, N. K., Weissleder, R., and Hilderbrand, S. A. (2008) Tetrazine-based cycloadditions: application to pretargeted live cell imaging. *Bioconjugate Chem. 19*, 2297−9.

(11) Pipkorn, R., Waldeck, W., Didinger, B., Koch, M., Mueller, G., Wiessler, M., and Braun, K. (2009) Inverse-electron-demand Diels-Alder reaction as a highly efficient chemoselective ligation procedure: synthesis and function of a BioShuttle for Temozolomide transport into prostate cancer cells. *J. Pept. Sci. 15*, 235−41.

(12) Patterson, D. M., Nazarova, L. A., Xie, B., Kamber, D. N., and Prescher, J. A. (2012) Functionalized cyclopropenes as bioorthogonal chemical reporters. *J. Am. Chem. Soc. 134*, 18638−43.

(13) Yang, J., Seckute, J., Cole, C. M., and Devaraj, N. K. (2012) Live-cell imaging of cyclopropene tags with fluorogenic tetrazine cycloadditions. *Angew. Chem., Int. Ed. 51*, 7476−9.

(14) Chen, W., Wang, D., Dai, C., Hamelberg, D., and Wang, B. (2012) Clicking 1,2,4,5-tetrazine and cyclooctynes with tunable reaction rates. *Chem. Commun. 48*, 1736−8.

(15) Karver, M. R., Weissleder, R., and Hilderbrand, S. A. (2012) Bioorthogonal reaction pairs enable simultaneous, selective, multi-target imaging. *Angew. Chem., Int. Ed. 51*, 920−2.

(16) Niederwieser, A., Spate, A. K., Nguyen, L. D., Jungst, C., Reutter, W., and Wittmann, V. (2013) Two-color glycan labeling of live cells by a combination of Diels-Alder and click chemistry. *Angew. Chem., Int. Ed. 52*, 4265−8.

(17) Carroll, L., Evans, H. L., Aboagye, E. O., and Spivey, A. C. (2013) Bioorthogonal chemistry for pre-targeted molecular imaging–progress and prospects. *Org. Biomol. Chem. 11*, 5772−81.

(18) Kettenbach, K., Schieferstein, H., and Ross, T. L. (2014) $^{18}$F-labeling using click cycloadditions. *Biomed. Res. Int. 2014*, 361329.

(19) Reiner, T., and Zeglis, B. M. (2014) The inverse electron demand Diels-Alder click reaction in radiochemistry. *J. Labelled Compd. Radiopharm. 57*, 285−90.

(20) Devaraj, N. K., Thurber, G. M., Keliher, E. J., Marinelli, B., and Weissleder, R. (2012) Reactive polymer enables efficient in vivo bioorthogonal chemistry. *Proc. Natl. Acad. Sci. U. S. A. 109*, 4762−7.

(21) Devaraj, N. K., Upadhyay, R., Haun, J. B., Hilderbrand, S. A., and Weissleder, R. (2009) Fast and sensitive pretargeted labeling of cancer cells through a tetrazine/*trans*-cyclooctene cycloaddition. *Angew. Chem., Int. Ed. 48*, 7013−6.

(22) Rossin, R., Lappchen, T., van den Bosch, S. M., Laforest, R., and Robillard, M. S. (2013) Diels-Alder reaction for tumor pretargeting: in vivo chemistry can boost tumor radiation dose compared with directly labeled antibody. *J. Nucl. Med. 54*, 1989−95.

(23) Rossin, R., Verkerk, P. R., van den Bosch, S. M., Vulders, R. C., Verel, I., Lub, J., and Robillard, M. S. (2010) In vivo chemistry for pretargeted tumor imaging in live mice. *Angew. Chem., Int. Ed. 49*, 3375−8.

(24) Zeglis, B. M., Sevak, K. K., Reiner, T., Mohindra, P., Carlin, S. D., Zanzonico, P., Weissleder, R., and Lewis, J. S. (2013) A pretargeted PET imaging strategy based on bioorthogonal Diels-Alder click chemistry. *J. Nucl. Med. 54*, 1389−96.

(25) Denk, C., Svatunek, D., Filip, T., Wanek, T., Lumpi, D., Frohlich, J., Kuntner, C., and Mikula, H. (2014) Development of a $^{18}$F-labeled tetrazine with favorable pharmacokinetics for bioorthogonal PET imaging. *Angew. Chem., Int. Ed. 53*, 9655−9.

(26) Herth, M. M., Andersen, V. L., Lehel, S., Madsen, J., Knudsen, G. M., and Kristensen, J. L. (2013) Development of a $^{11}$C-labeled tetrazine for rapid tetrazine-*trans*-cyclooctene ligation. *Chem. Commun. 49*, 3805−7.

(27) Li, Z., Cai, H., Hassink, M., Blackman, M. L., Brown, R. C., Conti, P. S., and Fox, J. M. (2010) Tetrazine-*trans*-cyclooctene ligation for the rapid construction of $^{18}$F labeled probes. *Chem. Commun. 46*, 8043−5.

(28) Liu, S., Hassink, M., Selvaraj, R., Yap, L. P., Park, R., Wang, H., Chen, X., Fox, J. M., Li, Z., and Conti, P. S. (2013) Efficient $^{18}$F




DOI: 10.1021/acs.bioconjchem.5b00089
*Bioconjugate Chem.* 2015, 26, 435−442

labeling of cysteine-containing peptides and proteins using tetrazine-*trans*-cyclooctene ligation. *Mol. Imaging 12*, 121−8.
(29) Selvaraj, R., Liu, S., Hassink, M., Huang, C. W., Yap, L. P., Park, R., Fox, J. M., Li, Z., and Conti, P. S. (2011) Tetrazine-*trans*-cyclooctene ligation for the rapid construction of integrin $\alpha_v\beta_3$ targeted PET tracer based on a cyclic RGD peptide. *Bioorg. Med. Chem. Lett. 21*, 5011−4.
(30) Wu, Z., Liu, S., Hassink, M., Nair, I., Park, R., Li, L., Todorov, I., Fox, J. M., Li, Z., Shively, J. E., et al. (2013) Development and evaluation of $^{18}$F-TTCO-Cys40-Exendin-4: a PET probe for imaging transplanted islets. *J. Nucl. Med. 54*, 244−51.
(31) Chen, X., Sievers, E., Hou, Y., Park, R., Tohme, M., Bart, R., Bremner, R., Bading, J. R., and Conti, P. S. (2005) Integrin $\alpha_v\beta_3$-targeted imaging of lung cancer. *Neoplasia 7*, 271−9.
(32) Liu, S., Li, Z., Yap, L. P., Huang, C. W., Park, R., and Conti, P. S. (2011) Efficient preparation and biological evaluation of a novel multivalency bifunctional chelator for $^{64}$Cu radiopharmaceuticals. *Chem.—Eur. J. 17*, 10222−5.
(33) Liu, S., Li, D., Park, R., Liu, R., Xia, Z., Guo, J., Krasnoperov, V., Gill, P. S., Li, Z., Shan, H., et al. (2013) PET imaging of colorectal and breast cancer by targeting EphB4 receptor with $^{64}$Cu-labeled hAb47 and hAb131 antibodies. *J. Nucl. Med. 54*, 1094−100.
(34) Liu, S., Li, D., Shan, H., Gabbai, F. P., Li, Z., and Conti, P. S. (2014) Evaluation of $^{18}$F-labeled BODIPY dye as potential PET agents for myocardial perfusion imaging. *Nucl. Med. Biol. 41*, 120−6.
(35) Liu, D. S., Tangpeerachaikul, A., Selvaraj, R., Taylor, M. T., Fox, J. M., and Ting, A. Y. (2012) Diels-Alder cycloaddition for fluorophore targeting to specific proteins inside living cells. *J. Am. Chem. Soc. 134*, 792−795.
(36) In a model study, the N-acetyl derivative of 6 was reacted with trans-cyclooctene. The initially formed dihydropyridazine product partially oxidized to the pyridazine on workup. After separation by column chromatography, the pyridazine could be isolated in pure form, but the dihydropyridazine product continued to slowly oxidize upon dissolution.
(37) The rate of reaction for a derivative of dipyridyltetrazine 3 with the equatorial diastereomer of 5-hydroxy-*trans*-cyclooctene is $k_2$ 5280 $M^{-1}$ $s^{-1}$ at 25 °C in 55:45 water:MeOH. See ref 6.
(38) Chen, X., Park, R., Shahinian, A. H., Tohme, M., Khankaldyyan, V., Bozorgzadeh, M. H., Bading, J. R., Moats, R., Laug, W. E., and Conti, P. S. (2004) $^{18}$F-labeled RGD peptide: initial evaluation for imaging brain tumor angiogenesis. *Nucl. Med. Biol. 31*, 179−89.
(39) Li, Z. B., Wu, Z., Chen, K., Chin, F. T., and Chen, X. (2007) Click chemistry for $^{18}$F-labeling of RGD peptides and microPET imaging of tumor integrin $\alpha_v\beta_3$ expression. *Bioconjugate Chem. 18*, 1987−94.


DOI: 10.1021/acs.bioconjchem.5b00089
*Bioconjugate Chem.* 2015, 26, 435−442